

Effect of Annealing on the Structural-phase State and Magnetoresistance of Three-layer Film Systems Based on Ni and V as well as Ni and Ag or Au

T.M. Grychanovs'ka, T.S. Kholod, O.A. Hrychanovs'ka, L.A. Tsygankova

Sumy State University, 2, Rimsky-Korsakov St., 40007 Sumy, Ukraine

(Received 11 January 2016; published online 15 March 2016)

The structural-phase state and magnetoresistive properties of three-layer film systems based on Ni and V and Ni and Au or Ag of the total thickness of $d = 25\text{-}55$ nm with the constant spacer thickness of $d_s = 5$ nm are studied. The influence of annealing temperatures from 300 to 600-700 K and the total thickness of the sample on the magnetoresistance value and behavior of the magnetoresistive dependences are experimentally tested. It is established that in the specified annealing temperature range the Ni/Ag/Ni film systems maintain negative isotropic magnetoresistance; Ni/Au/Ni samples have anisotropic magnetoresistance, and magnetoresistance of Ni/V/Ni film system is very sensitive to changes in the total thickness of the sample, i.e. it can have both the isotropic and anisotropic magnetoresistance.

Keywords: Structural-phase state, Magnetoresistance, Three-layer film system, Annealing.

DOI: [10.21272/jnep.8\(1\).01018](https://doi.org/10.21272/jnep.8(1).01018)

PACS numbers: 73.43.Qt, 75.70.Ak, 75.70.Cn

1. INTRODUCTION

Physical properties of different magnetic nanostructures take one of the leading places in modern scientific research in the field of solid state physics. Discovery of the giant magnetoresistance (GMR) effect in certain heterostructures [1-7] followed by the improvement of their electrical and magnetic characteristics allowed to reach significant values of the magnetoresistance at room temperature in weak magnetic fields [8-10]. Currently, the GMR effect is widely used in data processing and storage devices [11-13], spinners [14] and sensors [15, 16].

All the mentioned fields of application of thin-film elements require such a selection of the system components, at which roughness of the interface is minimal. The authors of [17, 18] studied the questions about the interface structure in metal systems based on Ni and V and Co and Cu and their electrophysical properties. The authors of [19] investigated the interface structure of Ag/Ni multilayers with low mutual solubility deposited by the ion beam in gaseous media (Ar) or by magnetron sputtering on different substrates. According to the data of [17-19], one can conclude that the behavior of the state diagrams of bulk samples cannot guarantee that the multilayer film system has stable and qualitative (with low roughness) interfaces. In spite of the fact that stability of the characteristics of film systems, such as magnetoresistance, is extremely important from the point of view of their practical application, then each thin-film system requires an additional study.

Three-layer spin-valve structures, in which the GMR and magnetoresistive effects are observed [20-25], are of great scientific interest. Usually, the composition of such structures includes, at least, two ferromagnetic layers separated by an ultrathin sublayer of a non-magnetic metal with high conductivity (spacer). A spacer prevents the direct exchange interaction of ferromagnetic layers. In this work, layers of 3d-ferromagnetic metal Ni were separated by the layer of non-ferromagnetic transition metal V, Ag or Au. On an example of Ni/V/Ni, Ni/Ag/Ni or Ni/Au/Ni three-layer film systems, we performed the experimental study of the magnetoresistive properties in combination with the establishment of the phase state

and impact of annealing. The investigation results will give the possibility to predict and control the operating characteristics of thin-film elements of the devices in the conditions of the size effect manifestation and influence of temperatures and magnetic fields.

2. EXPERIMENTAL

Ni, V, Ag, Au thin films and Ni/Au/Ni, Ni/Ag/Ni and Ni/V/N three-layer systems were manufactured by the thermal evaporation method in vacuum of $10^{-3}\text{-}10^{-4}$ Pa. The amorphous glass ceramic plates served as the substrates for the magnetoresistive studies. Layer-by-layer deposition of the materials was performed from two evaporators on the substrate at the temperature of 300 K. Thicknesses of individual layers were determined by the quartz resonator method. The samples were annealed in the temperature range from 300 to 600-700 K.

Magnetoresistance (MR) of the studied samples was measured at room temperature by the automated complex using the four-point scheme. This complex allows to automatically fix MR changes in thin-film systems in the longitudinal, transverse, and perpendicular measurement geometries. The MR values of film systems were calculated by the relation $(\Delta R/R_s) = (R(B) - R_s)/R_s$, where $R(B)$ and R_s are the sample resistance for the specified magnetic and saturation fields, respectively.

The electron microscopic and the electron diffraction investigations were carried out using TEM-125 K. The electron diffraction patterns of film materials were interpreted by the standard technique [26] using the reference of Al film. Calculation of the interplanar distances and determination of the lattice parameters were conducted with the accuracy of ± 0.001 nm by the ratios for crystals of the cubic syngony.

3. RESULTS AND DISCUSSION

3.1 Structural-phase state

The state diagram of the system based on Ni and V in the high-temperature part is rather complicated and is characterized by the presence of a number of intermediate phases (V_2Ni , VNi_3 , VNi_2 , and V_3Ni). Eutectics

and a number of solid solutions (s.s.) take also place in the Ni-V system. The lattice parameter increases from 0.3528 to 0.3625 nm in the s.s. based on the Ni lattice depending on the V content (concentration from 2.57 to 41.92 wt. %) [27]. Thus, the active phase formation processes, which will also influence the magnetoresistive properties of the samples, should be expected in the film systems. Based on the data of electron microscopic study, the phase composition in Ni(40 nm)/V(5 nm)/Ni(10 nm) three-layer film systems in the unannealed state corresponds to the bcc-V + fcc-s.s. (Ni, V) (Fig. 1a). The average parameters of the bcc-V and fcc-s.s. (Ni, V) lattices have the values \bar{a} (V) = 0.303-0.304 nm and \bar{a} (Ni) = 0.352-0.353 nm, which are close to the lattice parameters of single-layer films and bulk samples a_0 (V) = 0.3039 nm and a_0 (Ni) = 0.3523 nm [26]. Analysis of the micrographs showed that the films in the unannealed state are finely divided with the average crystallite size of 15-20 nm.

Annealing in the $300\text{ K} \leq T_{ann} \leq 600\text{ K}$ temperature range does not usually cause changes in the phase composition of the samples and significant recrystallization processes. However, the lines corresponding to the fcc-VO_x with $\bar{a} = 0.408\text{ nm}$ (Fig. 1b), where $x \approx 1$ (based on the dependence of the lattice parameter on the oxygen concentration) appear on the diffraction patterns of the samples of some Ni(40 nm)/V(5 nm)/Ni(10 nm) film systems [28]. The study of diffusion processes performed in [29] agrees well with the data of phase composition. In the film systems annealed in the $600\text{ K} \leq T_{ann} \leq 700\text{ K}$ range, one can observe an increase in the lattice parameter of Ni up to the values \bar{a} (Ni) = 0.353-0.354 nm that can be explained by the formation of the fcc-s.s. (Ni, V) with the average crystallites size of 25-30 nm based on the Ni crystal lattice. The content of vanadium atoms was equal to 4-10 wt. %. The estimation was carried out according to the dependence of the lattice parameter of s.s. (Ni-V) on the V concentration [27].

The state diagram of Au-Ni [27] shows that Au and Ni atoms have unlimited solubility in the liquid and, at high temperatures, in the solid states. Alloys of the Au-Ni system have the fcc-lattice. With increasing Ni fraction up to 37-46 wt. %, there occurs a decrease in temperatures of the crystallization start, and the minimum caused by the intersection of the liquidus and solidus curves at 1220 K appears on the diagram [27]. Decomposition of a homogeneous s.s. to a mixture of s.s. based on Au and Ni takes place when the alloy is cooled below 1100 K. Besides, components of the chosen system have the same crystal lattices, whose parameters significantly differ from each other and are equal to 0.4078 nm and 0.3523 nm for Au and Ni, respectively [27].

In the work, it is confirmed by the electron diffraction analysis that as-deposited Ni/Au(5 nm)/Ni samples of the total thickness of $d = 25\text{-}55\text{ nm}$ mostly do not preserve the individuality of separate layers. Two groups of lines corresponding to the fcc-Au (\bar{a} (Au) = 0.408 nm) and fcc-s.s. (Ni, Au) (\bar{a} (Ni) = 0.355 nm) are seen on the electron diffraction patterns. The films based on Ni and Au in the unannealed state are finely divided with the average size of crystallites of 5-10 nm, respectively. Annealing at 600 K does not cause the structural phase changes, and the samples remain biphasic. As seen from Fig. 1c, two sets of lines corresponding to the electron diffraction on the fcc-lattices of pure Au and fcc-s.s. (Ni, Au) hold. The

formation of a s.s. ($\bar{a} = 0.360\text{-}0.361\text{ nm}$) during the film deposition process was also fixed for Ni(5 nm)/Au(5 nm)/Ni(40 nm) samples, and in this case the sample can be considered biphasic fcc-Au + fcc-s.s. (Ni, Au). The lattice parameter increases from 0.3593 to 0.4035 nm in a s.s. based on Ni depending on the Au content in it (concentration from 10 to 90 wt. %) [27]. Thus, content of gold atoms in such s.s. was approximately equal to 15 wt. %.

Annealing of the Ni/Au(5 nm)/Ni samples in the temperature range of 300-700 K causes the convergence of Au and Ni lines that implies the formation of s.s. based on the components of the film system.

As the state diagram shows, Ag-Ni system is simple monotectic one. The maximum solubility of Ag in Ni is ~ 1 wt. % and decreases with decreasing temperature [30]. Two sets of lines corresponding to the fcc-Ni and fcc-Ag with the average lattice parameters \bar{a} (Ni) = 0.353 nm and \bar{a} (Ag) = 0.407 nm are present on the electron diffraction patterns of the as-deposited Ni/Ag(5 nm)/Ni film systems of the total thickness of $d = 25\text{-}55\text{ nm}$.

The average size of crystallites for the film systems based on Ni, Ag is equal to 30-40 nm. As Fig. 1d shows, annealing of the samples in the $300\text{ K} \leq T_{ann} \leq 600\text{ K}$ temperature range does not cause changes in the phase composition of the film system, but the reflexes become clearer that indicates an insignificant increase in the crystallites sizes. With further annealing in the temperature range of $600\text{ K} \leq T_{ann} \leq 700\text{ K}$, the film system retains the biphasic fcc-Ni + fcc-Ag composition with the lattice parameters, which are close to the tabulated data for bulk samples [26].

3.2 Magneto-resistive properties

The magneto-resistive measurements of several sets of unannealed and annealed in the temperature range from 300 to 600-700 K Ni/V/Ni, Ni/Au/Ni, and Ni/Ag/Ni film systems of the total thickness of $d = 25\text{-}55\text{ nm}$ with the constant spacer thickness of $d_s = 5\text{ nm}$ (Table 1) are performed in the present work. Thus, for one series of the samples with fixed thicknesses of the base Ni layer ($d_1 = 40\text{-}45\text{ nm}$) and spacer ($d_s = 5\text{ nm}$), thickness of free Ni layer d_2 was constant ($d_2 = 10\text{ nm}$), and for another series – varied in the range from 5 to 20 nm. The study of the influence on the MR value of the decrease in the total thickness of a three-layer sample at the constant spacer thickness (Table 1) was additionally carried out. In Fig. 2 we present the dependences of the longitudinal and transverse MR for unannealed film systems with the Ni layer thickness of $d_2 = 10\text{ nm}$ and different spacer materials. The analysis of the obtained data showed that isotropic MR of different magnitudes and opposite sign is observed for unannealed Ni/V/Ni and Ni/Ag/Ni film systems with $d_2 = 10\text{ nm}$ (Fig. 2). Thus, the maximum value of $\Delta R/R_s$ in the longitudinal geometry is equal to 0.16 % for the Ni(10)/V(5)/Ni(40) sample, and 0.57 % – for the Ni(10)/Ag(5)/Ni(40) sample, which is almost 4.5 times more in the absolute value (Fig. 2a). The feature of these dependences is the absence of clearly pronounced peaks that can indicate separate reversal of Ni layers. In our case, probably, due to different thicknesses of Ni layers ($d_1 = 40\text{ nm}$, $d_2 = 10\text{ nm}$) they have different coercivity that is confirmed by the blurring of the peaks. The same loops are observed for asymmetric structures,

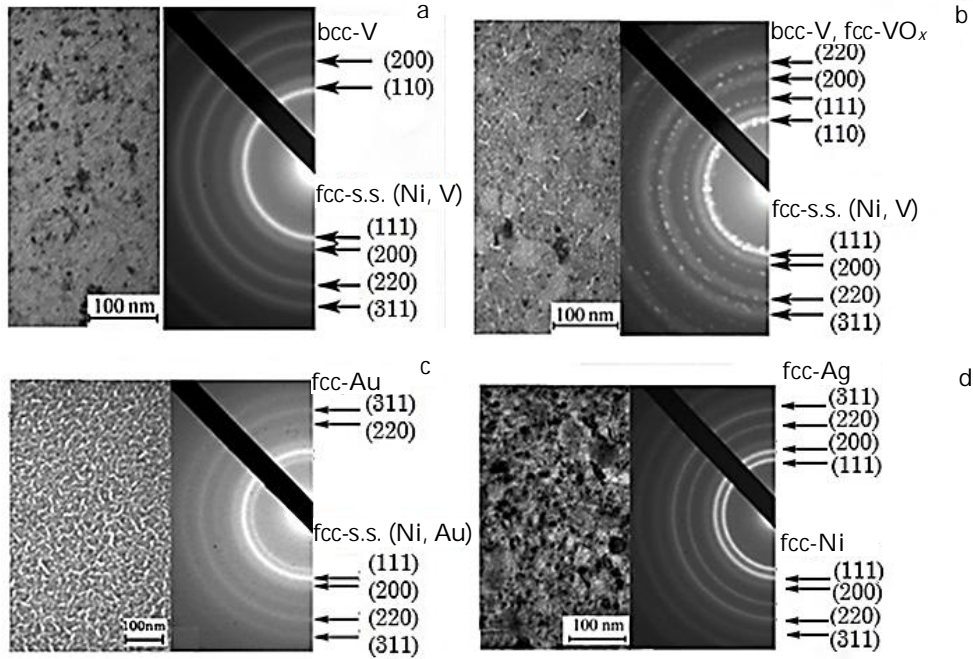


Fig. 1 – Diffraction pattern and crystal structure of the Ni(10)/V(5)/Ni(40)/Sub film system of as-deposited (a) and annealed to 600 K (b) and Ni(10)/Au(5)/Ni(40)/Sub (c) and Ni(10)/Ag(5)/Ni(40)/Sub (d) annealed to 600 K; Sub is the substrate, thickness in nm

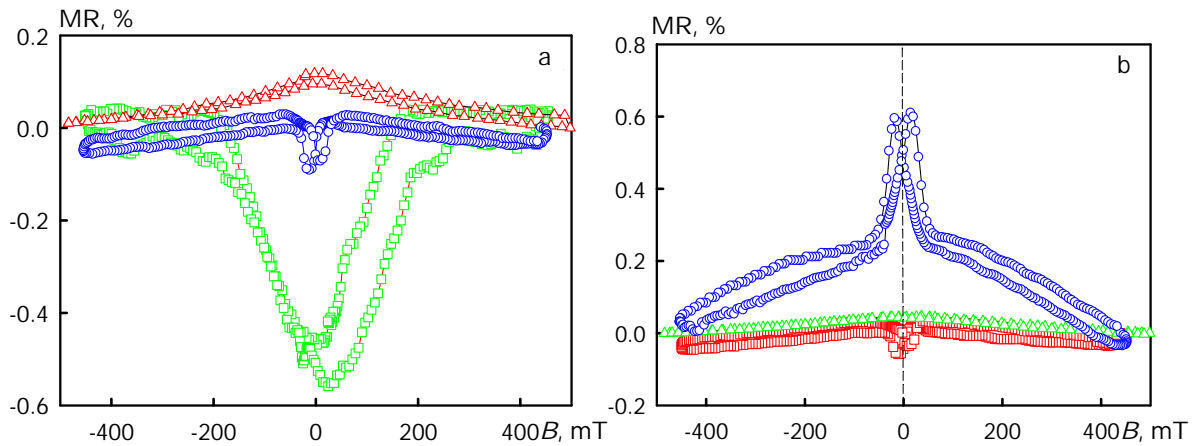


Fig. 2 – Field dependences of the longitudinal (a) and perpendicular (b) MR for the Ni(40)/Ag(5)/Ni(10) (\square), Ni(40)/V(5)/Ni(10) (Δ), and Ni(40)/Au(5)/Ni(10) (\circ) film systems

Table 1 – MR of unannealed and annealed film systems in two measurement geometries

No	Samples (nm)	$(\Delta R/R_s)_{\max}$, %			
		Longitudinal		Perpendicular	
		300 K	600 K	300 K	600 K
1	Ni(5)/Au(5)/Ni(15)/Sub	-0.12	-0.12	0.35	0.36
2	Ni(10)/Au(5)/Ni(15)/Sub	-0.12	-0.15	0.29	0.24
3	Ni(10)/Au(5)/Ni(40)/Sub	-0.14	-0.15	0.61	0.65
4	Ni(20)/Au(5)/Ni(20)/Sub	-0.06	-0.06	0.22	0.24
5	Ni(20)/Au(5)/Ni(30)/Sub	-0.11	-0.13	0.30	0.32
6	Ni(5)/Ag(5)/Ni(45)/Sub	-0.42	-0.44	-0.10	-0.13
7	Ni(10)/Ag(5)/Ni(40)/Sub	-0.57	-0.64	-0.06	-0.06
8	Ni(10)/V(5)/Ni(40)/Sub	0.16	0.16	0.06	0.051
9	Ni(10)/V(5)/Ni(45)/Sub	0.12	0.14	0.07	0.08

which are associated by the authors of [20] with the implementation of a stable antiferromagnetic distribution of the magnetization of ferromagnetic layers in a certain domain of the external magnetic field.

Anisotropic MR, whose magnitude and sign depend on the mutual orientation of the current in the sample and the external magnetic field, is observed for the Ni/Au/Ni system. The largest (in absolute value) values of $\Delta R/R_s$

for similar samples were observed in the perpendicular geometry and were equal to 0.6 % (Fig. 2b). Peaks of the magnetoresistive loops of the Ni/Au/Ni system are clear and are formed in a narrow range of the magnetic field ($\Delta B = 10\text{-}20$ mT) that implies synchronism of the reversal processes of both Ni layers. It can be assumed that due to the formation of a s.s. during condensation, the interfaces are blurred, and the antiparallel orientation of the magnetization in the adjacent Ni layers does not occur. Such film system can be represented as the three-layer Ni/Au + s.s. (Ni, Au)/Ni one. Moreover, the realization of the two-layer s.s. (Au-Ni)/Ni system, which is reversed as a whole, is also possible. Formation of s.s. causes an increase in the spacer resistance and is necessarily reflected on the behavior of the MR loops. Thus, the MR value of the Ni/Au/Ni samples decreases several times in the transition from the perpendicular to the transverse measurement geometry. For example, the MR decreases almost 5 times and is equal to 0.11 % for the Ni(10)/Au(5)/Ni(40) system. Such a sharp change in the MR value in the perpendicular geometry relative to the transverse one can be explained by "driving" of the electric current into the ferromagnet layers due to the increase in the spacer resistivity because of the formation of a s.s. Annealing of the samples at the temperature of 600-700 K leads to an insignificant increase in the MR, but the behavior of the loops remains (Fig. 3a).

For another series of the samples, where d_2 varied in the range from 5 to 20 nm, it is seen that when the upper layer thickness approaches the bottom layer thickness, the magnetoresistive loops have a slightly different view: increase or decrease in the resistance occurs in a narrow range of the magnetic field ($\Delta B = 5\text{-}10$ mT), and the narrow sharp maxima are observed. As noted above, this indicates the simultaneous reversal of both layers that is proper for symmetric structures composed of two identical layers with the same coercivity. The upper and lower magnetic layers, in this case, are switched simultaneously at one value of the external magnetic field.

The decrease in the total thickness of three-layer samples of the total thickness of $d = 25\text{-}55$ nm at constant spacer thickness ($d_s = 5$ nm) differently affects the MR of three-layer Ni/V/Ni, Ni/Au/Ni, and Ni/Ag/Ni systems. For example, one can consider film systems with the same total thickness $d = 30$ nm and identical thicknesses of the corresponding layers.

Thus, for the three-layer Ni(10)/V(5)/Ni(15) system, isotropy of the field dependences does not remain, and MR decreases to 0.05-0.08 %, while MR isotropy remains in the Ni(10)/Ag(5)/Ni(15) samples. Annealing of both samples at the temperature of 600-700 K does not influence the behavior of the dependences and MR value. Anisotropic MR remains in the Ni(10)/Au(5)/Ni(15) film system, but annealing at 700 K leads to changes in the behavior of the field dependences (Fig. 3b). Comparing the dependences of MR for the Ni(10)/Au(5)/Ni(40) (total thickness $d = 55$ nm) and Ni(10)/Au(5)/Ni(15) (total thickness $d = 30$ nm) systems, shown in Fig. 3, one can see that peaks lose their distinct character that indicates in favor of separate switching of Ni layers. The MR value substantially decreases to 0.36 %. But the common thing for both samples is that the perpendicular MR exceeds several times the longitudinal and transverse ones.

4. CONCLUSIONS

1. The electron diffraction studies of the structural-phase composition of three-layer film systems based on Ni and V and Ni and Au (or Ag) of the total thickness of 25-55 nm (spacer thickness $d_s = 5$ nm) indicate the different behavior of its dependence on the heat treatment regime. The film systems obtained by the thermal evaporation method in vacuum at the substrate temperature of $T_{sub} \approx 300$ K have the following phase composition: bcc-V + fcc-s.s. (Ni, V) with the average lattice parameter of a s.s. of 0.352-0.353 nm; fcc-Au + fcc-s.s. (Ni, Au) with the average lattice parameter of a s.s. based on Ni of 0.360-0.361 nm; fcc-Ni + fcc-Ag with the lattice parameters close to the tabulated values of bulk samples. The films based on Ni and V, Ni and Au in the unannealed state are finely divided with the average size of crystallites of 15-20 nm and 5-10 nm, respectively. Thermal annealing of the samples based on Ni and V, Ni and Au in the temperature range from 300 to 600-700 K causes the increase in the lattice parameter by 0.2-0.3 % and in the crystallites size by 30-40 %. As-deposited film systems based on Ni and Ag have the average size of crystallites of 30-40 nm, which increases during thermal annealing by 20-25 %. The structural-phase composition and lattice parameters of Ni and Ag remain constant with thermal annealing in the temperature range from 300 to 600-700 K.

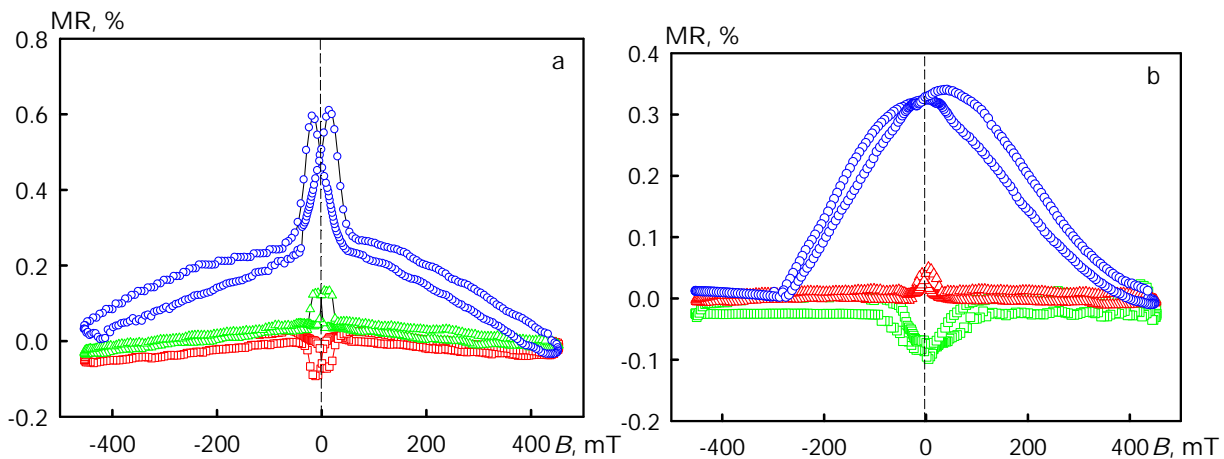


Fig. 3 – Field dependences of the MR of Ni(40)/Au(5)/Ni(10) (a) and Ni(15)/Au(5)/Ni(10) (b) film systems annealed to 700 K for three measurement geometries: longitudinal (\square); transverse (Δ); perpendicular (\circ)

2. The Ni/V/Ni and Ni/Ag/Ni film systems of the total thickness of 55 nm ($d_s = 5$ nm) have isotropic MR with the largest value in the parallel measurement geometry, but of the opposite sign. With decreasing total thickness of the Ni/V/Ni system to 30 nm, MR becomes anisotropic with the maximum value in the perpendicular measurement geometry. Annealing of the Ni/V/Ni and Ni/Ag/Ni samples at 600-700 K does not affect the behavior of the loops and MR magnitude.

3. The Ni/Au/Ni film systems have anisotropic MR. The maximum values of the MR are observed in the perpendicular measurement geometry and equal to 0.1 % for

the films of the total thickness of $d = 55$ nm and 0.5 % for the film of $d = 25$ nm. The MR value decreases 3-5 times with the transition from the perpendicular to the transverse orientation of the sample in an external magnetic field. The behavior of the loops and MR magnitude are changed with annealing of Ni/Au/Ni at 600-700 K.

ACKNOWLEDGMENTS

This work has been performed under the financial support of the Ministry of Education and Science of Ukraine (Grant No 0115U000689, 2015-2017).

REFERENCES

1. U. Hartman, *Magnetic Multilayers and Giant Magnetoresistance: Fundamentals and Industrial Applications* (Berlin: Heidelberg: New York: Springer-Verlag: 2000).
2. T.V. Ustinov, A.B. Rinkevich, L.N. Romashev, D. Perov, *Tech. Phys.* **49**, 613 (2004).
3. A.N. Stetsenko, V. Samofalov, V. Zorchenko, *JETP Lett.* **64**, 376 (1996).
4. F.S. Bergeret, A.F. Volkov, K.B. Efetov, *Rev. Mod. Phys.* **77**, 1321 (2005).
5. A.B. Svalov, P.A. Savin, G. Kurlandskaya, J. Gutiérrez, V.O. Vas'kovskiy, *Tech. Phys.* **47**, 987 (2002).
6. M. N. Baibich, J. M. Broto, A. Fert, F. Nguyen Van Dau, F. Petroff, P. Eitenne, G. Creuzet, A. Friederich, J. Chazelas, *Phys. Rev. Lett.* **61**, 2472 (1988).
7. P. Grünberg, R. Schreiber, Y. Pang, M.B. Brodsky, H. Sowers, *Phys. Rev. Lett.* **57**, 2442 (1986).
8. F. Pulizzi, *Nature Mater.* **11**, 367 (2012).
9. Claude Chappert, Albert Fert, Frédéric Nguyen Van Dau, *Nature Mater.* **6**, 813 (2007).
10. E. Hirota, H. Sakakima, K. Inomata, *Magneto-Resistance Devices* (Springer: 2002).
11. G.A. Prinz, *Science* **282**, 1660 (1998).
12. G.A. Prinz, *J. Magn. Magn. Mater.* **200**, 57 (1999).
13. J.F. Gregg, R.P. Borges, E. Jouguelet, C.L. Dennis, I. Petej, S.M. Thompson, K. Ounadjela, *J. Magn. Magn. Mater.* **265**, 274 (2003).
14. E.J. Torok, S. Zurn, L.E. Sheppard, R. Spitzer, Seongtae Bae, J.H. Judy, W.F.Jr. Egelhoff, P.J. Chen, *Magnetics Conference, 2002 (INTERMAG Europe 2002) art. no. 7473420* (Amsterdam: The Netherlands: 2007).
15. B. Anwarzai, V.Ac.S. Luby, E. Majkova, R. Senderak, *Vacuum* **84**, 108 (2010).
16. S. Luby, B. Anwarzai, V.Ac.E. Majkova, R. Senderak, *Vacuum* **86**, 718 (2012).
17. L. Odnodvoretz, S. Protsenko, O. Synashenko, D. Velykodnyi, I. Protsenko, *Cryst. Res. Technol.* **44**, 74 (2009).
18. M. Marzalek, A. Polit, V. Tokman, Y. Zabala, I. Protsenko, *Surface Sci.* **601**, 4454 (2007).
19. P. Sandström, E.B. Svedberg, M.P. Johansson, J. Birch, J.-E. Sundgren, *Thin Solid Films* **353**, 166 (1999).
20. M.H. Demydenko, S.I. Protsenko, D.M. Kostyuk, I.V. Cheshko, *J. Nano-Electron. Phys.* **3**, No 4, 81 (2011).
21. P. Sabareesan, M. Daniel, *J. Magn. Magn. Mater.* **324**, 4219 (2012).
22. Zhang Sun, Zichao Tang, Zhen Gao, *J. Molecular Structure* **1032**, 111 (2013).
23. H. Gokcan, J.C. Lodder, R. Jansen, *J. Mater. Sci. Eng. B* **126**, 129 (2006).
24. Jang-Hae Ku, Hyun Cheol Koo, Suk Hee Han, Jonghwa Eom, Gyutae Kimb, Joonyeon Chang, *Solid-State Electron.* **89**, 72 (2013).
25. Alain Schuhl, Daniel Lacour, *C.R. Physique* **6**, 945 (2005).
26. S.S. Gorelik, L.N. Rastorguev, Y. Skakov, *X-ray and electron graphical analysis of metals* (Moscow: GNTI: 1963).
27. A.M. Barabash, J.N. Kovalev, *Structure and properties of metals and alloys* (Kiev: Naukova Dumka: 1986).
28. Kh.Dzh. Gol'dshmidt, *Splavy vnedreniya, vyp. 1* (Moskva: Mir: 1971).
29. T.M. Grychanovska, A.M. Chornous, I.Yu. Protsenko, I.O. Shpetnyi, *Metallofiz. Nov. Technol.* **28** No 2, 267 (2006).
30. *Diagrammy sostoyaniya dvoynykh metallicheskih sistem. T.2* (Pod red. N.P. Lyakisheva) (Moskva: Mashinostroyeniye: 1997).